CAMBRIDGE
UNIVERSITY PRESS

RESEARCH ARTICLE

Relevance of shock waves derived from asteroid impacts in the atmosphere of the early Earth in the production of compounds of astrobiological interest

Luisa Ramírez-Vázquez[1] , Guadalupe Cordero-Tercero[1] , José de la Rosa[2] ,
Jorge Armando Cruz-Castañeda[2] and Alicia Negrón-Mendoza[2]

[1]Instituto de Geofísica, Universidad Nacional Autónoma de México, Mexico City, Mexico
[2]Instituto de Ciencias Nucleares, Universidad Nacional Autónoma de México, Mexico City, Mexico
Corresponding author: Guadalupe Cordero-Tercero; Email: gcordero@igeofisica.unam.mx

Abstract

The generation of organic compounds relevant to the origin of living beings is easily achieved if reducing conditions exist in the environment; however, proposed models of primitive atmospheres do not favour these conditions. This work considers the quantity and possible size of the cosmic bodies that could have impacted the Earth between 4.2 and 3.8 Ga. Different atmospheres (with gases such as CO_2, CO, N_2, CH_4) were experimentally irradiated by an Nd-YAG laser (used to simulate the energy of a shock wave produced by the interaction of a cosmic body with the atmosphere). Although the main products are short-chain, saturated and unsaturated hydrocarbons, hydrogen cyanide (HCN) is the most abundant in some atmospheres. HCN is an important precursor of the organic molecules relevant to chemical evolution. According to our calculations, between 10^{23} and 10^{25} g of HCN could have been produced by the energy released to the atmosphere from the entry of cosmic objects between 4.2 and 3.8 Ga. Therefore, this shock wave energy could play an important role in the processes of chemical evolution.

Contents

Introduction

Early atmosphere and chemical evolution

The atmosphere of terrestrial planets could have developed through processes such as nebular gas capture, from the volatiles from impactors during the accretion or post-accretion stages, and volcanic outgassing (Kuwahara and Sugita, 2015; Schaefer and Fegley, 2017). The atmospheric conditions of Earth in its first million years have not been determined due to the scarcity and limitations of geochemical and geological evidence (Marchi *et al*., 2016). However, Earth's atmosphere is described as a secondary atmosphere because the primary atmosphere was gravitationally captured gas from the solar nebula, which is composed mainly of hydrogen. This primordial atmosphere was lost and replaced by the secondary atmosphere, probably formed from volatiles delivered to Earth by asteroids, comets and volcanic emissions. The primitive atmosphere was probably dominated by CO_2, N_2 and H_2O (Zahnle *et al*., 2010; Kasting, 2018), and would have been a weakly reducing atmosphere.

Although models of the physiochemical characteristics of the atmospheric and terrestrial surface of the Hadean and early Archean eons are still debated, some evidence, such as the geochemistry of the oldest zircons (dated between 4.3–4.4 Ga), suggests that rocks were altered by liquid water at this time (Mojzsis *et al*., 2001; Zahnle, 2006). Analysis shows that they formed in fayalite-magnetite-quartz environments similar to the current mantle oxidation state, suggesting the state of the mantle has not changed significantly; however, the composition and redox state of a planet mantle are related to the chemistry of its atmosphere (Trail *et al*., 2011; Itcovitz *et al*., 2022). Despite the luminosity of the early Sun being lower than today (20–30%) (Sagan and Mullen, 1972; Kasting *et al*., 1984), zircons require liquid water to form; the hydrosphere existed on Earth by 4.3 Ga ago (Mojzsis *et al*., 2001). The greenhouse effect is necessary for liquid water to exist, even if the possible sources of gases such as CH_4 are difficult to explain. Elevated amounts of CO_2 and CH_4 are also necessary to explain the Young Sun paradox ($pCH_4 = 0.01$–10 mbar) (Charnay *et al*., 2020).

Understanding the atmospheric composition of the early Earth is essential for the studies related to prebiotic chemistry and the origin of life since the generation of the organic compounds relevant to living beings is easily achieved under reduced conditions, as Oparin (1924) and Urey (1952) proposed and as was observed in Miller's work (Miller, 1953).

Some mechanisms that contribute to the presence of CH_4 and H_2 in the atmosphere have been proposed: serpentinization at hydrothermal vents on the sea floor (Reeves and Fiebig, 2020), and chondritic material, given that asteroid impacts would have contributed to the formation of the secondary atmosphere due to the degassing of volatile compounds from the incoming asteroidal or cometary material. Theoretical studies have shown that primitive atmospheres would contain significant amounts of reducing species (CH_4, H_2) if they originate from chondritic material (Hashimoto *et al*., 2007; Schaefer and Fegley, 2007, 2010); and the reducing potential of large impacts (Kuwahara and Sugita, 2015; Benner *et al*., 2020; Zahnle *et al*., 2020; Itcovitz *et al*., 2022). In the latter case, many of the impactors are in a much more reduced state than the mantle. For example, many meteorites (including ordinary chondrites and enstatites) contain substantial amounts of metallic iron and iron sulphides, so the gases balanced with these materials would be highly reducing (Zahnle *et al*., 2020). Zahnle's *et al*.'s work (2020) supposes a greater contribution to the generation of CH_4 by considering >100 km diameter projectiles that could have collided with Earth during the late accretion. Large impacts would have contributed to obtaining a transient reduced environment due to the production of H_2 through the reduction of H_2O by the metallic iron from the impactor (Genda *et al*., 2017; Benner *et al*., 2020; Zahnle *et al*., 2020; Itcovitz *et al*., 2022*)*. After cooling, the atmosphere would have reduced conditions from the presence of CH_4 and NH_3. From these kinds of reduced molecules, it is possible to obtain HCN, an essential precursor of other molecular species relevant for prebiotic chemistry. Itcovitz *et al*. (2022) have found in their model that as the mass of the impactor increases, the production of H_2 also increases, and H_2 would be more abundant than CO_2, and the production of CO is expected. They also found that small amounts of CH_4 can be produced in the most reducing atmospheres, and the amount N_2 does not change significantly with impactor mass. Considering the

probable age of the formation of the Moon and the record of impact craters on its surface, it has been concluded that there was a high rate of impacts of asteroidal and cometary material between 4.5 and 3.5 Ga, which suggests that similar impacts also occurred on the surface of the Earth (Marchi *et al.*, 2016; Zellner, 2017). The lunar crater record also shows that the flux and size of the impactors decreased drastically after this period, the end of which seems to coincide with the origin of life (Farmer, 2000; Hartman *et al.*, 2000).

The studies focused on proposing pathways of prebiotic chemical reactions for the subsequent origin of life mostly involve scenarios on continental or oceanic crust. Some authors have considered the energy contribution of the shock waves produced by the passage of asteroids through the atmosphere to model or simulate the production of abiotic organic compounds. Bar-Nun *et al.* (1970) have produced chemical reactions in a mixture of gases (CH_4, C_2H_6, NH_3 and Ar) simulating primordial conditions and inducing shock waves. Their results show that amino acids such as glycine and alanine can be obtained. McKay and Borucki (1997) have used a laser to simulate the interaction of shock waves with an atmosphere composed of CH_4, H_2O, CO_2, N_2 and H_2S and one composed of H_2 and CO_2. They detected hydrogen cyanide (HCN), formaldehyde (HCHO), ethane (C_2H_6) and methylamine in the first simulated atmosphere and water and CO in the second. Shock waves in the Martian atmosphere have also been proposed as a mechanism for nitrogen fixation in the early stage of this planet (Navarro-González *et al.*, 2019).

In this work, we propose different models of primitive atmospheres, with and without a nitrogen source, and observe the possible role of shock waves from asteroid impacts on the atmosphere in producing relevant organic compounds for the chemical evolution on Earth.

Methodology

Theoretical calculations of impact energy

The energy of the shock waves produced by the passage of asteroids through the atmosphere of Earth could have produced compounds of astrobiological interest. We assessed the energy this kind of shock wave produced to determine how much energy could have been released and how many compounds could have been produced. Due to plate tectonics and weathering, the record of impact craters on the surface of the Earth has been obliterated, so the number and size of past impacts are unknown. However, the surface of the Moon can be used to estimate these parameters.

Possible early life indicators are presumed to be found in seafloor precipitates of hydrothermal vents and could be as old as 3.7 Ga (Dodd *et al.*, 2017). Also, some structures can provide data on the dates of the presence of pristine life: stromatolites, which are defined by Schopf (2006) as 'accretionary sedimentary structures, commonly thinly layered, megascopic and calcareous, inferred to have been formed by mat-building communities of mucilage-secreting microorganisms, mainly photoautotrophic microbes'. Furthermore, sedimentary structures provide information about the environments where they were formed, that is, in shallow waters. The stromatolites discovered in the Isua greenstone belt have dated to ~3.7 Ga (Nutman *et al.*, 2016, 2019). However, it has also been suggested that these structures are probably not of biological origin, so there is still a debate about these systems (Allwood *et al.*, 2018). We are concerned about the chemical evolution period, i.e. the time before life became widespread. The period of interest in this study is before the first unambiguous forms of life (3.7 Ga). In this work, 3.8 Ga was the lower limit.

Figure 3 in Halliday (2006) shows that the Moon was formed between 40 and 50 Ma after the solar system began to form. After the impact of Gaia and Theia, the surface of the Moon was a magma ocean that eventually hardened into the crust. Carlson *et al.* (2014) have performed isotopic analysis of several lunar rocks to assess the age of the crust. According to this analysis, the crustal rocks have formation ages between 4.32 and 4.50 Ga. The youngest age they reported was 4283 ± 23 Ma, although this could be due to the behaviour of the plagioclase, on which their results depend. On this basis, 4.2 Ga was the upper limit for assessing the number of impacts over the Moon and the Earth. This date range

Table 1. *Number of impact craters that must have been produced on the Moon and the Earth between 4.2 and 3.8 Ga*

Diameter (km)	Number of craters on the Moon	Number of craters on the Earth
1.1	847 544	11 441 848–28 223 226
1.5	248 205	3 350 765–8 265 220
2.2	80 197	1 082 658–2 670 557
3.0	29 260	395 012–974 362
4.3	12 221	164 984–406 961
6.1	5938	80 165–197 740
8.6	3443	46 476–114 641
12.2	2376	32 077–79 122
17.2	1794	24 223–59 751
24.4	1300	17 552–43 296
34.4	818	11 046–27 248
48.7	429	5793–14 291
68.9	189	2555–6301
97.4	73	991–2444
137.8	27	361–891
194.8	10	133–328
275.5	4	53–130

The third column shows the range of impact crater populations that could have been formed on the Earth if the impact flux was between 13.5 and 33.3 times the impact flux on the Moon

ensures that the period under consideration includes the presence of a lunar (and hence an impact record) and the time before life appeared on Earth.

Neukum *et al.* (2001) have stated that the temporal dependence of the number of craters ≥1 km in diameter per km^2 of surface area is represented by the equation:

$$N(\geq 1) = 5.44 \; x \; 10^{-14} \; [\exp{(6.93T)} - 1] + 8.38 \; x \; 10^{-4} \; T \tag{1}$$

where T is the crater accumulation time in Ga. Integrating equation (1) between 3.8 and 4.2 Ga and multiplying by the Moon's surface area (~37 962 900 km^2 assuming an equatorial radius of 1738.1 km), around 1 233 834 impact craters ≥1 km were produced in this time interval.

On the other hand, Neukum *et al.* (2001) have also represented the size-frequency distribution of lunar craters (their equation (2)), i.e. the number of craters with a diameter greater than D formed per km^2 during 1 Ga as a polynomial of degree 11. This equation is valid for craters with diameters between 0.01 and 300 km. This polynomial keeps its shape for every interval of time. To consider the constraints of equation (1) and those of this polynomial, only craters whose diameters were between 1 and 300 km were considered. In this context, the shape of the polynomial and the result from the previous paragraph were used to calculate the number of craters of different sizes formed on the Moon between 4.2 and 3.8 Ga.

To do this, we normalize the number of impact craters with a diameter ≥1 km and multiply the result by 1 233 834. Then, to have a non-accumulated distribution function, we subtract the value of one interval from the previous one. Our results are in Table 1. There, the diameter, D, in the first column, is equal to $\sqrt{D_L D_R}$, where D_L is the lower limit, and D_R is the upper limit of the interval, as in Neukum *et al.* (2001). In this study, we started with a diameter of 0.01 km, but in Table 1, we consider only the interval between 905 m and 327 km.

Table 2. *Number of impact craters that could have formed on the crust of the Earth between 4.2 and 3.8 Ga and the putative energies that the entry of the impactors could have released to the atmosphere, assuming that the number of impacts on Earth was 13.5 times greater than the number of impacts on the Moon*

Diameter (km)	Number of craters on the Earth (lower limit)	Kinetic energy of one impact J	Kinetic energy of all impacts $\times 10^{27}$ J	1% of the energy released by all impacts $\times 10^{25}$ J
1.1	11 441 848	5.1×10^{20}	5.8	5.8
1.5	3 350 765	1.3×10^{21}	4.3	4.3
2.2	1 082 658	4.1×10^{21}	4.4	4.4
3.0	395 012	1.0×10^{22}	4.1	4.1
4.3	164 984	3.0×10^{22}	5.0	5.0
6.1	80 165	8.7×10^{22}	6.9	6.9
8.6	46 476	2.4×10^{23}	11.3	11.3
12.2	32 077	6.9×10^{23}	22.2	22.2
17.2	24 223	1.9×10^{24}	47.1	47.1
24.4	17 552	5.5×10^{24}	97.4	97.4
34.4	11 046	1.6×10^{25}	171.7	171.7
48.7	5793	4.4×10^{25}	255.5	255.5
68.9	2555	1.2×10^{26}	319.2	319.2
97.4	991	3.5×10^{26}	349.7	349.7
137.8	361	1.0×10^{27}	360.8	360.8
194.8	133	2.8×10^{27}	375.5	375.5
275.5	53	8.0×10^{27}	423.3	423.3
Total				**2464.2**

According to Canup and Asphaug (2001), the ratio of impact rate of the Moon to that of the Earth is

$$N_1 = \frac{f_M R_M^2}{f_E R_E^2} \qquad (2)$$

where R_E is the radius of the Earth, R_M is the radius of the Moon, and f_M and f_E are the gravitational focusing factors of the Moon and Earth, respectively. N_1 can have values between 0.03 and 0.074; that is, in the same time interval, between 13.5 and 33.3 times more impact craters could have been produced on the Earth than on the Moon (Table 1).

According to Table 1, between 4.2 and 3.8 Ga, at least 546 cosmic objects with diameters D, such that $115 \text{ km} < D < 328 \text{ km}$, fell on Earth. The impacts of such objects could have contributed to generating CH_4.

Based on Table 1, the energy released in the atmosphere due to the entry of cosmic bodies can be assessed. Globally, 95.1% of falls are stony meteorites, of which 93.1% are chondrites, of which 93.9% are ordinary chondrites (Korotev, 2021). This means that 83.1% of the falls are ordinary chondrites. In first approximation, impactors before 3.8 Ga are compositionally similar to present-day impactors; thus, the most common material that has impacted the Earth is ordinary chondrite, whose mean density is 3.54 g cm^{-3} (Britt and Consolmagno, 2003). The mean impact velocity of asteroids on our planet is 20.3 km s^{-1} (Brown *et al.*, 2002). Therefore, the energy of each object in Table 1 was calculated using the equation for the kinetic energy and assuming that the objects are spheres. The results obtained are shown in the third column of Tables 2 and 3. The fourth column of these tables shows the total entry energies due to all the impactors of each size that fell into the atmosphere of the Earth between 4.2 and 3.8 Ga.

Table 3. *Number of impact craters that could have formed on the crust of the Earth between 4.2 and 3.8 Ga and the putative energies that the entry of the impactors could have released to the atmosphere, assuming that the number of impacts on Earth was 33.3 times greater than the number of impacts on the Moon*

Diameter (km)	Number of craters on the Earth (upper limit)	Kinetic energy of one impact J	Kinetic energy of all impacts $\times 10^{28}$ J	1% of the energy released by all impacts $\times 10^{26}$ J
1.1	28 223 226	5.1×10^{20}	1.4	1.4
1.5	8 265 220	1.3×10^{21}	1.1	1.1
2.2	2 670 557	4.1×10^{21}	1.1	1.1
3.0	974 362	1.0×10^{22}	1.0	1.0
4.3	406 961	3.0×10^{22}	1.2	1.2
6.1	197 740	8.7×10^{22}	1.7	1.7
8.6	114 641	2.4×10^{23}	2.8	2.8
12.2	79 122	6.9×10^{23}	5.5	5.5
17.2	59 751	1.9×10^{24}	11.6	11.6
24.4	43 296	5.5×10^{24}	24.0	24.0
34.4	27 248	1.6×10^{25}	42.4	42.4
48.7	14 291	4.4×10^{25}	63.0	63.0
68.9	6301	1.2×10^{26}	78.7	78.7
97.4	2444	3.5×10^{26}	86.2	86.2
137.8	891	1.0×10^{27}	89.0	89.0
194.8	328	2.8×10^{27}	92.6	92.6
275.5	130	8.0×10^{27}	103.8	103.8
Total				**607.1**

A portion of this energy is transformed into heat energy, which increases the temperature of the incoming body, melting and evaporating part of its material. As the body continues moving, only a part of its pre-entry kinetic energy is deposited in the atmosphere. The Earth Impact Effects Program is an interactive website that permits users to estimate several effects of the impact of a cosmic body on Earth (https://impact.ese.ic.ac.uk/ImpactEarth/ImpactEffects/). According to this program, an object with a diameter of 905 m, density of 3540 kg m^{-3}, velocity of 20.3 km s^{-1} and an entry angle of 45° (the most probable angle) will lose ~1.2% of its entry energy in the atmosphere. This program does not give this information for more massive objects, possibly because the energy loss is lower. In this work, 1% of the entry energy is a reasonable upper limit for the energy deposited into the atmosphere due to the objects in Tables 2 and 3 (fifth column of both tables).

Considering the total energy released into the atmosphere by impactors >29 km (diameters ≥34.4 km in Table 2), they are responsible for 91.5% of the energy released into the atmosphere by all the impactors that hit the Earth in the time interval of interest. Considering that the larger the object, the less energy is deposited in the atmosphere, we could put an even greater restriction and consider only objects smaller than 29 km. In this case, the total energy deposited in the atmosphere (adding the first 10 rows from the fifth column of Tables 2 and 3) was between 2.1×10^{27} and 5.1×10^{27} J.

The work of Pérez-Rodríguez (2020) is similar to this section, as it is a compilation of various works that simulate the effect of a shock wave in atmospheres with different proposed compositions (Table 4).

Based on Table 4, and as an example, 1 J of energy produces 10^{16} molecules of NO in a neutral atmosphere, so if all the energy released by impactors that hit Earth between 4.2 and 3.8 Ga was used to produce this compound, then 2.46×10^{44}–6.07×10^{44} molecules of NO, i.e. 1.2×10^{22}–3.0×10^{22} g of NO, could have been formed during this period. If we consider our more restrictive values (2.1×10^{27} and 5.1×10^{27}), the number of molecules formed was between 2.1×10^{43} and

Table 4. *Studies of the production of organic molecules in the atmosphere. Their energy sources simulate those of shock waves*

Authors	Type of test	Atmospheric composition	Experimental conditions or assumptions	Compounds	Results Production (molecules J^{-1})
Bar-Nun et al. (1970)	Experiment	**Reduced** 3.3% CH_4 11% C_2H_6 5.6% NH_3 80.1% Ar	$E = 4 \times 10^{11}$ erg mol^{-1} =40000 J mol^{-1} T: 2000–4000 K	Amino acids	1.1×10^{18}
Chameides and Walker (1981)	Model	**Reduced** N H C O C/O≈1	$E = 10^5$ J mol^{-1} T:2000–5000 K	HCN	10^{16}
	Model	**Neutral** N H C O C/O≈0	$E = 10^5$ J mol^{-1} T:2000–5000 K	NO	10^{16}
McKay and Borucki (1997)	Experiment	**Reduced** H_2O 42% CO_2 29% CH_4 22% N_2 4.3% H_2S 3.7%	$T = 2500$ K $E = 2$ J	C_2H_2, HCN, C_6H_4 CH_3NH_2, C_2H C_2, $C_2N_2H_4$, CO_2H_2, $C_2O_2H_4$, C_6H_6, S_2 HCHO CH_3SH C_2H_6 C_2H_4	5.0×10^{17} 10^{17} 5.0×10^{16} 2.0×10^{16} 1.0×10^{16} 2.0×10^{14} 5.0×10^{14}
	Experiment	**Reduced** H_2 2/3 CO_2 1/3	$T = 2500$ K	H_2O and CO	5.0×10^{16}
Navarro et al. (2019)	Experiment	**Neutral** CO_2 H_2 N_2 $0 < \alpha^1 < 1$	$T = 17000$ K $V = 60$ km s^{-1} $P = 1$ bar $E = 6.42 \times 10^{10}$ J	NO	$\alpha = 0.01$ 4.9×10^{13} $\alpha = 0.80$ 1.3×10^{16} $\alpha = 0.98$ 1.9×10^{15}

Taken from Pérez Rodríguez (2020).
[1]$\alpha = CO_2/(CO_2 + N_2)$

5.1×10^{43}, or equivalently between 1.0×10^{21} and 2.5×10^{21} g of NO. From these preliminary results, we decided to perform an experimental study of the simulated released energy by a shock wave in different models of primitive atmospheres.

Table 5. *Nitrogen-free atmospheres used in the first set of experiments*

| Irradiation time (min)	Atmosphere
30	50% CO_2
	50% CH_4
30	50% CO_2
	48% CH_4
	2% H_2
30	50% CO_2
	20% CO
	20% CH_4
	10% H_2
60	42% CH_4
	38% CO_2
	20% H_2
60	50% CO_2
	25% CO
	10% H_2O
	10% CH_4
	5% H_2
90	65% CO_2
	32% CO
	3% H_2
90	96% CO_2
	2% CO
	2% H_2
180	50% CO_2
	50% CH_4
300	90% CO_2
	10% CH_4

Experimental procedure

The methodology was divided into three sections. The first set of experiments consisted of the laser irradiation of different gas mixtures (including CO, CO_2, H_2O and CH_4) without a nitrogen source (details in Table 5) to evaluate the possibility of obtaining oxygenated compounds (e.g. alcohols, carboxylic acids) relevant to chemical evolution. The second set of experiments consisted of preparing CH_4, CO_2 and N_2 atmospheres, varying the content of the last two gases, and keeping a constant 1 h irradiation time (see Table 6) to observe the differences among the products obtained in the first set of experiments. The third set was the analysis of a particular atmosphere from second set at different irradiation times to study the production yield of the relevant compounds. All experiments were performed in triplicate.

Reactor filling system and simulated atmosphere irradiation

High-purity gases ($CO_2 = 99.99\%$, $CH_4 = 99.97\%$, $N_2 = 99.99\%$, $CO = 99.99\%$) were used to simulate primitive atmospheres and were supplied by Praxair, Inc. The cylinders were connected to a two-step regulator and a filter. The gas flowed through a stainless-steel pipe to a mixing system, where the atmospheres to be simulated were prepared. The mixer used was a Linde FM-4660, equipped with an Omega DP-350 temperature gauge, a Combitron CM 351 vacuum gauge and an Omega DP-80

Table 6. *Composition of the simulated atmospheres for the second set of experiments*

Atmospheres with nitrogen
10% N_2, 10% CH_4, 80% CO_2
30% N_2, 10% CH_4, 60% CO_2
40% N_2, 10% CH_4, 50% CO_2
50% N_2, 10% CH_4, 40% CO_2
60% N_2, 10% CH_4, 30% CO_2
70% N_2, 10% CH_4, 20% CO_2
80% N_2, 10% CH_4, 10% CO_2
85% N_2, 10% CH_4, 5% CO_2
88% N_2, 10% CH_4, 2% CO_2
90% N_2, 10% CH_4
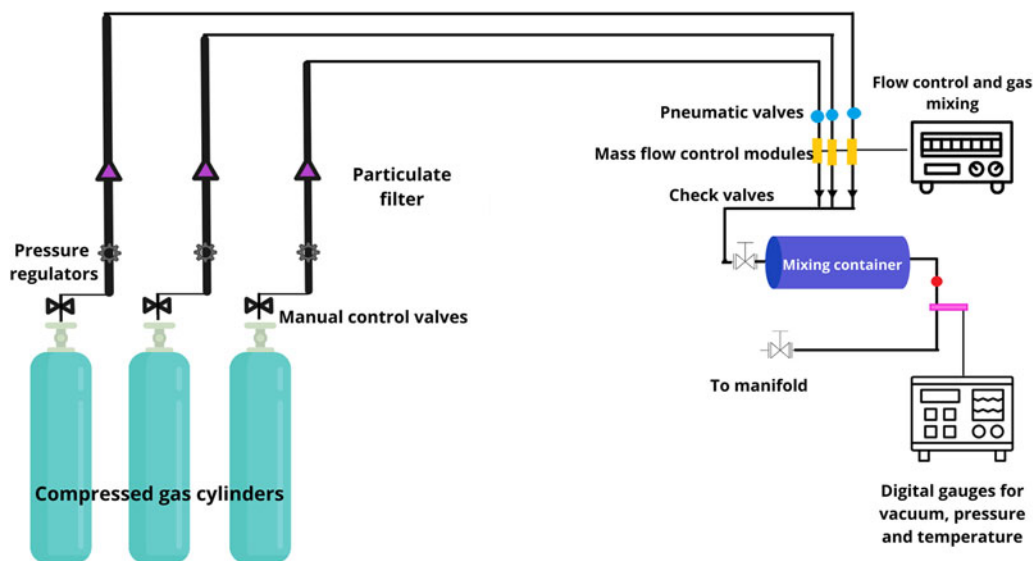
Figure 1. *Experimental setting (adapted from Segura and Navarro-González, 2005).*

temperature gauge. It has eight electronic channels that control and measure gas mass flow through thermal conductivity (each channel supports a different gas). All the experiments were realized in the Plasma Chemistry and Planetary Studies Laboratory at the Nuclear Sciences Institute (ICN), UNAM. Figure 1 shows the experimental setting for preparing the gas mixture.

The containers for the gaseous mixtures were spherical Pyrex glass flasks (1000 mL) with a high vacuum Teflon valve with 3 O-rings adapted; this tap allows the connection to fill the container. Once filled, the container was placed on the optical table for irradiation. The laser was a solid-state Nd-YAG with pulsed laser energy of 7 ns and a wavelength of 1.06 nm. The laser produces a short-duration plasma, as well as high temperatures and pressures, which can simulate the energetic process of a shock wave. The energy deposited into the system was determined by the difference between the input laser energy and the transmitted energy and was determined using a LabMaster model LM ULTIMA power and energy measurement system.

Analysis of samples

Gas products

An Agilent 7890a gas chromatograph with a six-port automatic injection system linked to a 2 mL pneumatic injection circuit was used for the chemical analysis and separation of the irradiation products. The temperature programme used for separating the compounds was initially operated at 50 °C for 5 min and continued at a temperature ramp of 10 °C per minute until the final temperature of 240 °C was reached. The carrier gas used was helium (grade ultra-high purity 99.999%), with a split ratio of 10:1 and a split flow of 120 mL min^{-1}. The separation column was a fused silica capillary CP-PorabondQ of 50 m length, 0.32 mm internal diameter and a stationary phase thickness of 5 mm. After chromatographic separation, the products were analysed using an Agilent 5975C inert XL EL/CI MSD mass spectrometer with a quadrupole Triple-Axis detector. The electronic impact mode was used, with a spectral interval of 10–100 m/z and a resolution of 1 amu. The compounds were identified through SCAN mode or mass scanning and compared with the NIST 05 Mass spectral library, to detect the compounds that are generated after irradiation.

Solid product

The solid residue produced after the irradiation of some samples (details in section 'Chemical analysis of the organic polymers') was collected with methanol and later evaporated and analysed by different techniques:

Attenuated total reflectance-Gourier transform infrared ATR-FTIR spectroscopy

A Spectrum 100 Perkin Elmer® spectrophotometer was used. The sample was analysed using 20 scans. The interval between 400 and 4000 cm^{-1} was selected for the acquired spectra.

Raman spectroscopy analysis

An Optosky ATR 3000 portable Raman spectrometer was used with a Class IIIB laser positioned at an operating distance of 6 mm from the sample, and the laser was kept at a constant value of 400 mW. A NaCl window was used for the analysis. Raman and FTIR spectroscopy were performed at the Department of Radiation Chemistry and Radiochemistry at the ICN-UNAM.

Elemental analysis

A Perkin Elmer PE2400 Analyser was used for duplicated sample analysis of the percentile content of carbon, hydrogen and nitrogen. The carrier gas utilized was helium. The temperature of the chromatographic column was set at 82.2 °C, with a thermal conductivity detector. The combustion reactor was set at 975 °C and the reduction reactor at 501 °C. The analysis time was 430 s, and the calibration compound used was cystine. This analysis was conducted at the Research and Industry Support Services Unit (USAI) at the Faculty of Chemistry, UNAM.

Results

Atmospheres without a nitrogen source

All the atmospheres prepared were irradiated between 0.5 and 5 h. The gas composition of those mixtures is summarized in Table 7. Generally, the compounds obtained after irradiation were short-chain, saturated and unsaturated hydrocarbons (C2–6). No oxygenated compounds (i.e. alcohols, ethers, carboxylic acids, etc.) were found at the experimental conditions used in this study.

CO_2, CH_4 and N_2 atmospheres

Short-chain hydrocarbons were also produced in the nitrogen-containing atmospheres (Table 8); different molecules were produced as the CO_2 content decreased. In the mixtures with a more significant amount of nitrogen (≥80% N_2), the formation of organic polymers as yellowish solids deposited on

Irradiation time (min)	Atmosphere	Compound	Production (molecules J^{-1})
30	50% CO_2	Acetylene	1.1×10^{20}
	50% CH_4	Ethane	1.7×10^{19}
		Propene	2.7×10^{18}
		Propane	6.1×10^{17}
		Propyne	1.4×10^{19}
		1-Butene	8.5×10^{17}
		1-Buten-3-yne	8.3×10^{18}
		2-Butyne	2.09×10^{18}
		1,3-Butadiyne	2.4×10^{19}
		Benzene	1.2×10^{19}
30	50% CO_2	Acetylene	9.9×10^{19}
	48% CH_4	Ethane	1.1×10^{19}
	2% H_2	Propene	2.4×10^{18}
		Propane	5.3×10^{17}
		Propyne	1.3×10^{19}
		1-Butene	7.8×10^{17}
		1-Buten-3-yne	7.3×10^{18}
		2-Butyne	1.9×10^{18}
		1,3-Butadiyne	2.2×10^{19}
		Benzene	7.8×10^{18}
30	50% CO_2	Acetylene	5.9×10^{19}
	20% CO	Ethane	6.5×10^{18}
	20% CH_4	Propene	1.4×10^{18}
	10% H_2	Propane	3.3×10^{17}
		Propyne	3.2×10^{18}
		1-Butene	4.8×10^{17}
		1-Buten-3-yne	3.7×10^{18}
		2-Butyne	9.7×10^{17}
		1,3-Butadiyne	1.0×10^{19}
		Benzene	3.1×10^{18}
60	42% CH_4	Acetylene	1.5×10^{20}
	38% CO_2	Ethane	7.3×10^{18}
	20% H_2	Propene	3.6×10^{18}
		Propane	3.6×10^{17}
		Propyne	2.4×10^{19}
		1-Butene	7.4×10^{17}
		1-Buten-3-yne	1.8×10^{19}
		2-Butyne	1.9×10^{18}
		1,3-Butadiyne	7.8×10^{19}
		Benzene	5.0×10^{19}
60	50% CO_2	Ethylene	2.2×10^{19}
	25% CO	Ethane	4.8×10^{18}
	10% H_2O	Propene	7.4×10^{17}
	10% CH_4	Propane	3.4×10^{17}
	5% H_2	Propyne	1.4×10^{18}
		1-Butene	2.3×10^{17}

(*Continued*)

Table 7. (*Continued.*)

Irradiation time (min)	Atmosphere	Compound	Production (molecules J^{-1})
		1-Buten-3-yne	8.2×10^{17}
		1-Butyne	2.0×10^{17}
		1,3-Butadiyne	1.2×10^{18}
		Benzene	1.4×10^{18}
90	65% CO_2 32% CO 3% H_2	No products were detected	---
90	96% CO_2 2% CO 2% H_2	No products were detected	---
180	50% CO_2 50% CH_4	Acetylene	1.14×10^{20}
		Ethane	2.25×10^{19}
		Propene	1.1×10^{19}
		Propane	2.8×10^{18}
		Propyne	1.2×10^{19}
		1-Butene	2.9×10^{18}
		1-Buten-3-yne	8.6×10^{17}
		2-Butyne	2.1×10^{19}
		1,3-Butadiyne	3.9×10^{18}
		Benzene	1.6×10^{19}
300	90% CO_2 10% CH_4	No products were detected	---

the walls of the reactors was observed. Compounds containing two carbons were detected from the 60% N_2, 10% CH_4 and 30% CO_2 atmosphere and appeared in each subsequent atmosphere. Compounds containing three carbons or more carbons were detected in the gas mixture corresponding to 80% N_2, 10% CH_4 and 10% CO_2. Figure 2 shows a chromatogram from the 88% N_2, 10% CH_4 and 2% CO_2 mixture after 1 h of irradiation.

Chemical analysis of the organic polymers

We collected the yellowish solid produced after irradiation and obtained the ATR-FT-IR and Raman spectra of the sample (Fig. 3). Both spectra show that compounds with the expected functional groups are present. The results are consistent with previous analyses of tholins (Mutsukura and Akita, 1999; Imanaka *et al.*, 2004; Quirico *et al.*, 2008; Mendoza-Téllez, 2022) but include additional bands corresponding to C=O or C–OH bands due to the CO_2 present in the original gas mixture.

Elemental analysis shows that low amounts of nitrogen are present in the solid sample obtained after the irradiation of the 85% N_2, 10% CH_4 and 5% CO_2 atmosphere (Table 9). The total elemental percentage is far from 100%. This discrepancy may be attributed to the presence of oxygenated compounds. Given that CO_2 was included in the gas mixture, the formation of oxygenated compounds in the precipitate post-irradiation is plausible. Previous research (Mendoza-Téllez, 2022) has established through pyrolysis and gas chromatography that the principal constituents of the yellowish precipitate—referred to as tholins, which emerge following the irradiation of N_2, CH_4 and CO_2—encompass aromatic hydrocarbons, nitrogenous compounds (e.g. acetonitrile, cyanoacetylene) and oxygen-containing compounds (e.g. methanol, ketones). These results also match the C=O and C–O–H bands in Fig. 3. A

Table 8. *Simulated atmospheres for the second set of experiments and the products obtained after irradiation*

Atmosphere	Produced compounds	Production (molecules J^{-1})
10% N_2, 10% CH_4, 80% CO_2	---	---
30% N_2, 10% CH_4, 60% CO_2	---	---
40% N_2, 10% CH_4, 50% CO_2	---	---
50% N_2, 10% CH_4, 40% CO_2	---	---
60% N_2, 10% CH_4, 30% CO_2	Acetylene	$5.1 10^{18}$
	Ethane	1.7×10^{18}
70% N_2, 10% CH_4, 20% CO_2	Acetylene	6.2×10^{18}
	Ethane	1.2×10^{18}
80% N_2, 10% CH_4, 10% CO_2	Acetylene	1.3×10^{19}
	Ethylene	1.2×10^{18}
	Ethane	1.8×10^{18}
	Propene	6.1×10^{17}
	Propane	6.7×10^{17}
	Propyne	2.4×10^{17}
	Hydrogen cyanide	3.4×10^{17}
	1,3-Butadiyne	7.6×10^{17}
85% N_2, 10% CH_4, 5% CO_2	Acetylene	2.1×10^{19}
	Ethylene	1.4×10^{18}
	Ethane	1.6×10^{18}
	Propene	1.0×10^{18}
	Propane	5.3×10^{17}
	Propyne	5.3×10^{17}
	Hydrogen cyanide	6.5×10^{18}
	1-Butene	2.7×10^{17}
	1-Buten-3-yne	7.6×10^{17}
	1,3-Butadiyne	2.7×10^{17}
	Benzene	4.7×10^{17}
88% N_2, 10% CH_4, 2% CO_2	Acetylene	2.5×10^{19}
	Ethylene	1.2×10^{18}
	Ethane	1.3×10^{18}
	Propene	1.0×10^{18}
	Propane	3.3×10^{17}
	Propyne	6.3×10^{17}
	Hydrogen cyanide	1.1×10^{19}
	1-Butene	3.1×10^{17}
	1-Buten-3-yne	1.2×10^{18}
	1-Butyne	3.5×10^{17}
	1,3-Butadiyne	5.6×10^{18}
	Benzene	7.8×10^{17}
90% N_2, 10% CH_4	Acetylene	2.3×10^{19}
	Ethylene	1.1×10^{18}
	Ethane	1.2×10^{18}
	Propene	1.1×10^{18}
	Propane	4.6×10^{17}
	Propyne	6.3×10^{17}
	Hydrogen cyanide	1.3×10^{19}

(*Continued*)

Table 8. (*Continued.*)

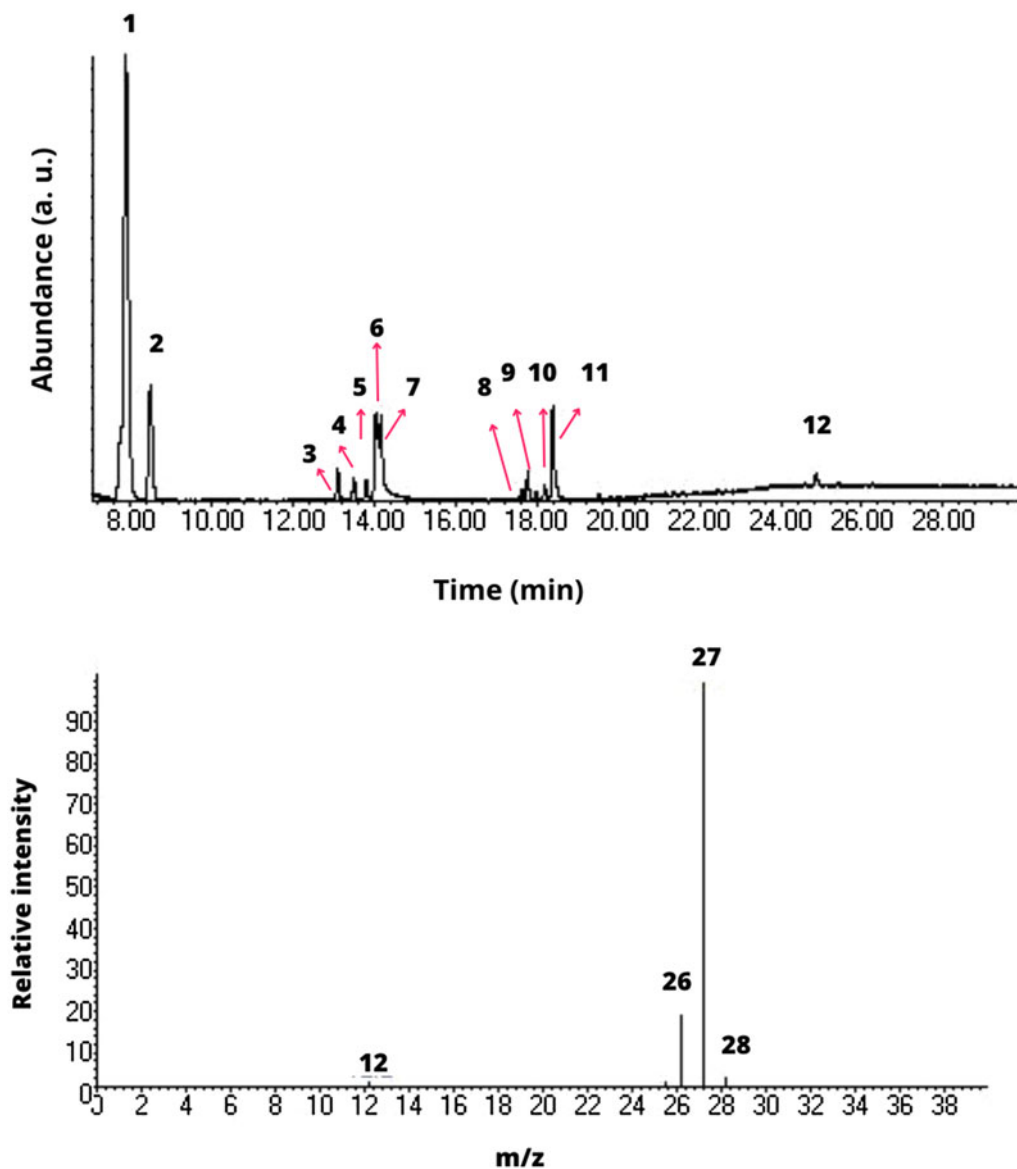| Atmosphere	Produced compounds	Production (molecules J^{-1})
	1-Butene	2.9×10^{17}
	1-Buten-3-yne	1.3×10^{18}
	1-Butyne	3.3×10^{17}
	1,3-Butadiyne	6.5×10^{18}
	Benzene	8.6×10^{17}

Figure 2. *Above: Chromatogram (scan mode) of the irradiation products of the 88% N_2, 10% CH_4 and 2% CO_2 atmosphere, where HCN is separated from the other hydrocarbons produced (peaks: (1) ethylene; (2) ethane; (3) propene; (4) propane; (5) propyne; (6) hydrogen cyanide; (7) propyne; (8) 1-butene; (9) 1-buten-3-yne; (10) 1-butyne; (11) 1,3-butadiyne; (12) benzene). Below: CG-MS spectra of the analysed hydrogen cyanide.*
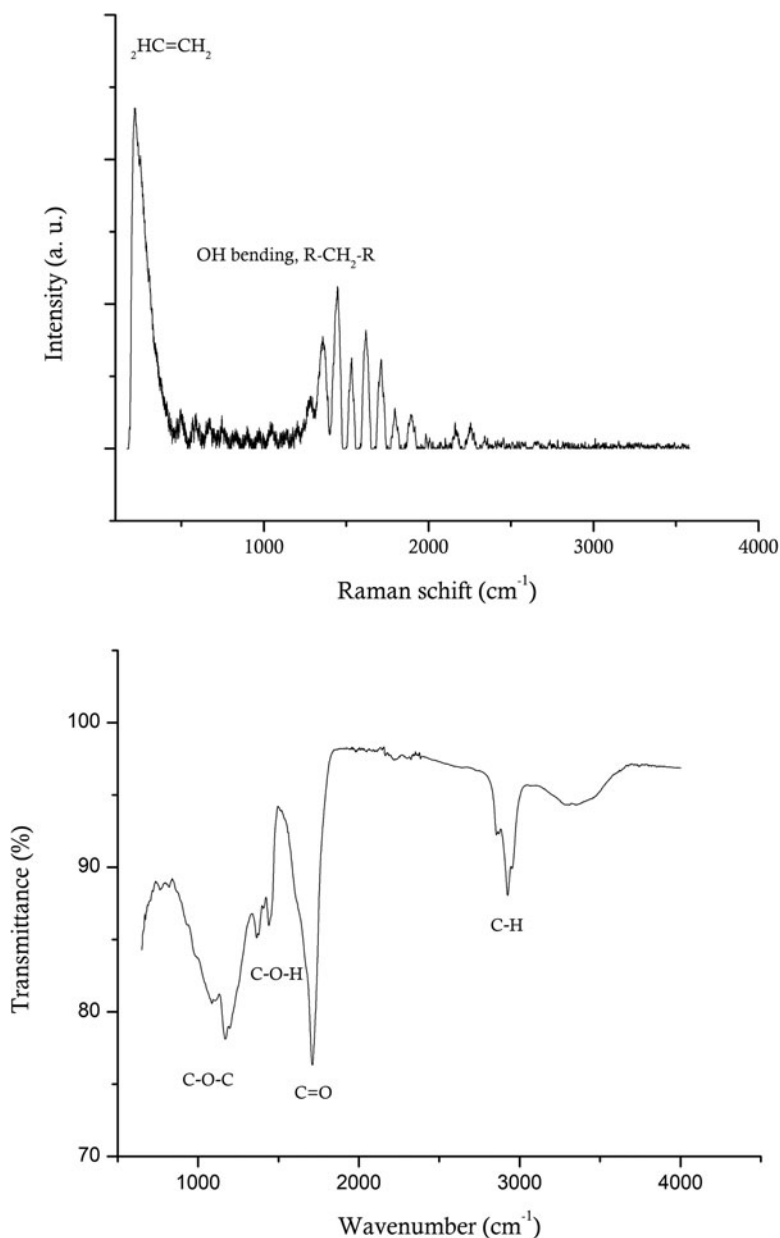
Figure 3. *Above: Raman spectrum of the remnant solid after the irradiations. Below: Infrared spectrum of the same sample. The solid sample was obtained after the irradiation (1 h) of the 85% N_2, 10% CH_4 and 5% CO_2 mixture.*

Table 9. *Elemental analysis of the solid sample (obtained after 1 h irradiation of 85% N_2, 10% CH_4 and 5% CO_2 mixture)*

Analysed sample (mg)	% Carbon	% Hydrogen	% Nitrogen
1.931	66.82	6.69	3.11
2.110	66.43	6.63	3.18
Average	66.625	6.660	3.145

Results are represented as percentages by weight. The instrument's limit of quantification was 1% for C, H, N and S.

Production of HCN in the 85% N_2, 10% CH_4, 5% CO_2 atmosphere
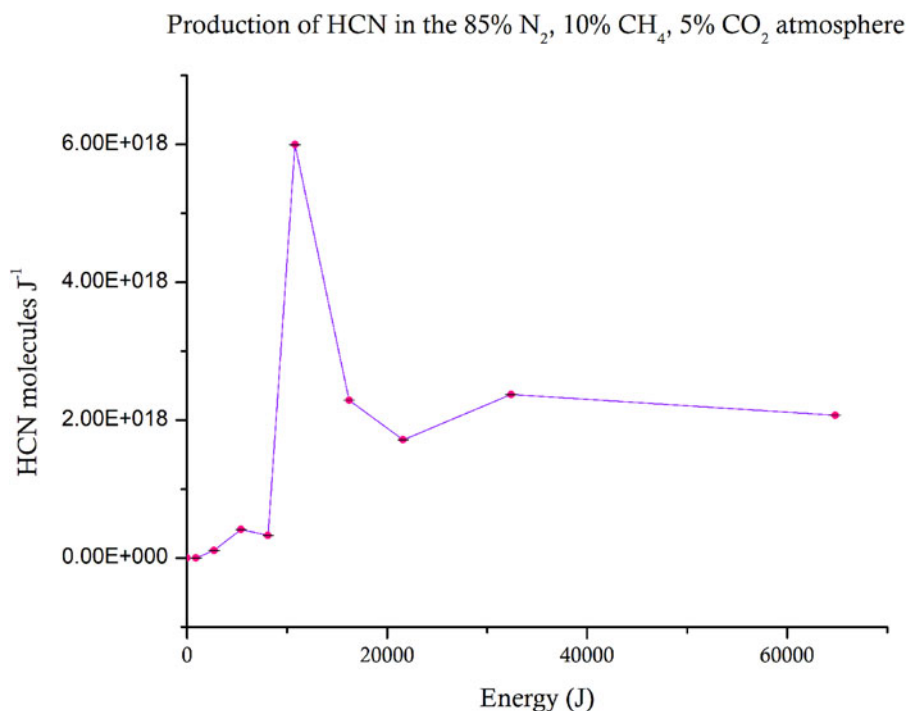
Figure 4. *Effect of the duration of irradiation on a simulated primitive Earth atmosphere. The sample conditions were: 300 mJ per pulse, 1000 mbar and a frequency of 10 Hz.*

potential explanation for the emergence of oxygenated compounds within the precipitates is the thermal dissociation of CO_2, yielding CO and O_2 (Navarro-González *et al.*, 2001). Consequently, oxygen may become available for the synthesis of organic compounds, such as ketones. A comprehensive analysis and elucidation of the mechanisms underlying tholin production are beyond the scope of this work.

Production of HCN in relation to the simulated energy from shockwaves

The 85% N_2, 10% CH_4 and 5% CO_2 atmosphere was selected to study the production of HCN at different laser irradiation times (between 0 and 6 h). The exposure time of the simulated early Earth atmosphere was converted into dissipated energy by multiplying the exposure time by the pulse energy (300 mJ) of the laser irradiation to obtain the HCN formation rate due to the energetic discharge of the laser in molecules per unit of energy. Figure 4 shows the HCN production relative to the dissipated energy. At the longest irradiation time (6 h, corresponding to 64 800 J) a low abundance of cyanoacetylene was observed among the irradiation products.

According to Fig. 4, the number of HCN molecules produced per J increases until it reaches a maximum at 10 000 J; after that, the number of molecules decreases and then remains almost constant for larger energies. Considering the most optimistic value (6×10^{18} molecules J^{-1}), 1.5×10^{47}–3.6×10^{47} molecules of HCN could have been formed by the release of shock energy into the atmosphere, if we consider the totals in Tables 2 and 3, or 1.3×10^{46}–3.1×10^{46} molecules of HCN if we consider our more restrictive values. This implies that, in the first case, between 6.6×10^{24} and 1.6×10^{25} g of HCN could have been formed or, in the second case, between 5.7×10^{23} g and 1.4×10^{24} g of HCN could have been formed. The mass of the Earth is 5.97×10^{27} g; thus, the estimated amount of HCN that could be produced is 0.26% of the mass of the Earth at most.

Discussion

The results obtained for the atmospheres proposed in the first set of experiments (section 'Atmospheres without a nitrogen source') show that hydrocarbons can be formed due to irradiation. Although these compounds do not have great relevance for prebiotic chemistry, it is assumed that the formation of other possibly relevant compounds is inhibited due to the presence of carbon dioxide. Other authors (Bar-Nun and Shaviv, 1975; Scattergood *et al.*, 1989; Sugisaki *et al.*, 1994; McKay and Borucki, 1997; Ferus *et al.*, 2020) have observed the possible effects of impacts on the atmosphere in the production of organic compounds, and have also produced hydrocarbons and HCN, despite starting with different gas mixtures of similar composition.

Although the atmospheric composition of the early Earth is still a matter of debate, one of several proposals is that the early atmosphere resembled the current atmospheric conditions of Titan (Clarke and Ferris, 1997; Trainer *et al.*, 2006), for example, their similar isotopic ratios of H, C, N and O suggest a possible cometary origin of Earth atmosphere (Trigo-Rodriguez and Martín-Torres, 2012). The presence of an organic haze would have contributed to protecting photo-dissociable compounds, such as methane and ammonia (Sagan and Chyba, 1997). If the atmosphere of the primitive Earth were dense, organic haze and meteoric metals would have acted as catalysts for forming complex organic molecules from methane and CO_2. Therefore, the atmosphere of Titan is a system we can consider understanding possible prebiotic pathways for forming relevant organic compounds on early Earth (Trigo-Rodriguez and Martín-Torres, 2012). The atmospheres chosen in this work (sections 'CO_2, CH_4 and N_2 atmospheres' and 'Production of HCN in relation to the simulated energy from shockwaves') are similar to that of Titan.

The results show that as the percentage of CO_2 in the mixtures decreases, the production of organic compounds is favoured, and even HCN is produced. HCN is essential for chemical evolution because it can be a precursor (through other prebiotic reactions) to molecules such as RNA and early proteins. Another compound of interest for prebiotic chemistry is cyanoacetylene; this molecule was obtained at the maximum irradiation of the 85% N_2, 10% CH_4 and 5% CO_2 gas mixture. This compound is a common electric discharge product on a methane–nitrogen mixture. It is also relevant to prebiotic chemistry because it can be a precursor of compounds such as cytosine, aspartic acid and asparagine (Orgel, 1998).

Conclusions

The results of subjecting these samples of possible primitive atmospheres to a simulation of the energy released by the shock waves produced by impactors of asteroidal and cometary material show that if the oxidizing character of the atmosphere is dominant, the production of organic compounds is diminished. Even so, they were produced in the atmospheres (Table 7) containing $\leq 10\%$ CO_2.

The energy released into the atmosphere by the impactors that hit the Earth between 4.2 and 3.8 Ga before the present could have provided the energy to produce organic compounds that could have played an important role in the chemical evolution period, such as HCN and NO. Although the estimates made in this work are upper limits and the atmospheres considered were favourable to their formation, the possible quantity of these compounds, which is equivalent to a few per cent of the mass of the Earth, should be considered. In the future, evaluating the dynamics of the reaction of the different compounds produced could be important.

While the Young Sun paradox seems to indicate that due to the lower luminosity of the Sun in its early years promoting very low temperatures on the early Earth, geological evidence, such as the dating of zircons mentioned above, indicates that the Earth had favourable conditions for chemical evolution and the subsequent origin of life. For this to be possible, greenhouse gases, such as CO_2 and CH_4, are necessary; compounds like CH_4 and NH_3 can be rapidly photolysed and would not accumulate in high enough concentrations to prevent freezing ocean water (Bada, 2004). Furthermore, there were no apparent sources of methane on the primitive Earth. However, this work shows that large impacts would be major contributors to the presence of this compound and cause transient reduced atmospheres. Around

546 cosmic objects with diameters >115 km could have impacted our planet during its first 700 Ma of history, providing multiple opportunities for these conditions. The energy released to the atmosphere by the entry of such a cosmic body could have produced between 5.7×10^{23} and 1.6×10^{25} g of HCN.

Author contributions. G. C.-T. derived the theory and L. R.-V. and J. d. l. R. performed the simulations. All authors contributed equally to analysing data, writing the manuscript and reaching conclusions.

Competing interest. None.

References

Allwood AC, Rosing MT, Flannery DT, Hurowitz JA and Heirwegh CM (2018) Reassessing evidence of life in 3,700-million-year-old rocks of Greenland. *Nature* **563**, 241–244.

Bada JL (2004) How life began on Earth: a status report. *Earth and Planetary Science Letters* **226**, 1–15.

Bar-Nun A and Shaviv A (1975) Dynamics of the chemical evolution of Earth's primitive atmosphere. *Icarus* **24**, 197–210.

Bar-Nun A, Bar-Nun N, Bauer SH and Sagan C (1970) Shock synthesis of amino acids in simulated primitive environments. *Science* **168**, 4–6.

Benner SA, Bell EA, Biondi E, Brasser R, Carell T, Kim H, Mojzsis SJ, Omran A, Pasek MA and Trail D (2020) When did life likely emerge on earth in an RNA9-first process? *ChemSystemsChem* **2**, e1900035.

Britt DT and Consolmagno SJGJ (2003) Stony meteorite porosities and densities: a review of the data through 2001. *Meteoritics and Planetary Science* **38**, 1161–1180.

Brown P, Spalding RE, ReVelle DO, Tagliaferri E and Worden SP (2002) The flux of small near-earth objects colliding with the earth. *Nature* **420**, 294–296.

Canup RM and Asphaug E (2001) Origin of the Moon in a giant impact near the end of the Earth's formation. *Nature* **412**, 708–712.

Carlson RW, Borg LE, Gaffney AM and Boyet M (2014) Rb-Sr, Sm-Nd and Lu-Hf isotope systematics of the lunar Mg-suite: the age of the lunar crust and its relation to the time of Moon formation. *Philosophical Transactions of the Royal Society A: Mathematical, Physical and Engineering Sciences* **372**, 20130246.

Chameides WL and Walker JCG (1981) Rates of fixation by lightning of carbon and nitrogen in possible primitive atmospheres. *Origins of Life* **11**, 291–302.

Charnay B, Wolf ET, Marty B and Forget F (2020) Is the faint young sun problem for earth solved? *Space Science Reviews* **216**, 90.

Clarke DW and Ferris JP (1997) Chemical evolution on Titan: comparisons to the prebiotic earth. *Origins of Life and Evolution of the Biosphere* **27**, 225–248.

Dodd MS, Papineau D, Grenne T, Slack JF, Rittner M, Pirajno F, O'Neil J and Little CTS (2017) Evidence for early life in Earth's oldest hydrothermal vent precipitates. *Nature* **543**, 60–64.

Farmer JD (2000) Hydrothermal systems: doorways to early biosphere evolution. *GSA Today* **10**, 1–9.

Ferus M, Rimmer P, Cassone G, Knízek A, Civiš S, Šponer JE, Ivanek O, Šponer J, Saeidfirozeh H, Kubelík P, Dudzák R, Petera L, Juha L, Pastorek A, Křivková A and Krůs M (2020). One-pot hydrogen cyanide-based prebiotic synthesis of canonical nucleobases and glycine initiated by high-velocity impacts on early earth. *Astrobiology* **20**, 1476–1488.

Genda H, Brasser R and Mojzsis SJ (2017) The terrestrial late veneer from core disruption of a lunar-sized impactor. *Earth and Planetary Science Letters* **480**, 25–32.

Halliday AN (2006) The origin of the earth what's new? *Elements* **2**, 205–210.

Hartman WK, Ryder G, Done L and Grinspoon D (2000) The time-dependent intense bombardment of the primordial earth/moon system. In Canup R and Righter K (eds), *Origin of the Earth and Moon*. Tucson, AZ: University of Arizona Press, pp. 493–512.

Hashimoto GL, Abe Y and Sugita S (2007) The chemical composition of the early terrestrial atmosphere: formation of a reducing atmosphere from CI-like material. *Journal of Geophysical Research E: Planets* **112**, 1–12.

Imanaka H, Khare BN, Elsila JE, Bakes ELO, McKay CP, Cruikshank DP, Sugita S, Matsui T and Zare RN (2004) Laboratory experiments of Titan tholin formed in cold plasma at various pressures: implications for nitrogen-containing polycyclic aromatic compounds in Titan haze. *Icarus* **168**, 344–366.

Itcovitz JP, Rae ASP, Citron RI, Stewart ST, Sinclair CA, Rimmer PB and Shorttle O (2022) Reduced atmospheres of post-impact worlds: the early earth. *The Planetary Science Journal* **3**, 115.

Kasting JF (2018) Atmosphere on early earth and its evolution as it impacted life. In Kolb VM (ed.), *Handbook of Astrobiology*. Boca Raton, FL: CRC Press, pp. 207–214. https://doi.org/10.1201/b22230-17

Kasting J, Pollack J and Crisp D (1984) Effects of high CO_2 levels on surface temperature and atmospheric oxidation state of the early Earth. *Journal of Atmospheric Chemistry* **1**, 403–428.

Korotev RL (2021) Some meteorite information. Available at https://sites.wustl.edu/meteoritesite/items/some-meteorite-statistics/

Kuwahara H and Sugita S (2015) The molecular composition of impact-generated atmospheres on terrestrial planets during the post-accretion stage. *ICARUS* **257**, 290–301.

Marchi S, Black BA, Elkins-Tanton LT and Bottke WF (2016) Massive impact-induced release of carbon and sulfur gases in the early Earth's atmosphere. *Earth and Planetary Science Letters* **449**, 96–104.

McKay CP and Borucki WJ (1997) Organic synthesis in experimental impact shocks. *Science* **276**, 390–392.

Mendoza-Téllez S (2022) Estudio de la generación de aerosoles oxigenados en una atmósfera simulada de Titán [Universidad Nacional Autónoma de México]. Available at http://132.248.9.195/ptd2022/noviembre/0832580/Index.html

Miller SL (1953) A production of amino acids under possibly primitive earth conditions. *Science* **117**, 528–529.

Mojzsis SJ, Harrison TM and Pidgeon RT (2001) Oxygen-isotope evidence from ancient zircons for liquid water at the Earth's surface 4,300 Myr ago sources and may therefore provide information about the nature. *Nature* **409**, 178–181.

Mutsukura N and Akita K (1999) Infrared absorption spectroscopy measurements of amorphous CN. *Thin Solid Films* **349**, 115–119.

Navarro-González R, McKay CP and Mvondo DN (2001) A possible nitrogen crisis for Archaean life due to reduced nitrogen fixation by lightning. *Nature* **412**, 61–64.

Navarro-González R, Navarro KF, Coll P, McKay CP, Stern JC, Sutter B, Archer PD, Buch A, Cabane M, Conrad PG, Eigenbrode JL, Franz HB, Freissinet C, Glavin DP, Hogancamp JV, McAdam AC, Malespin CA, Martín-Torres FJ, Ming DW, Morris RV, Prats B, Raulin F, Rodgriguez-Manfredi JA, Szopa C, Zorzano-Mier M-P, Mahaffy PR, Atreya S, Trainer MG and Vasavada AR (2019) Abiotic input of fixed nitrogen by bolide impacts to gale crater during the Hesperian: insights from the Mars Science Laboratory. *Journal of Geophysical Research: Planets* **124**, 94–113.

Neukum G, Ivanov BA and Hartmann WK (2001) Cratering records in the inner solar system in relation to the lunar reference system. *Space Sciences Reviews* **96**, 55–86.

Nutman AP, Bennett VC, Friend CRL, Van Kranendonk MJ and Chivas AR (2016) Rapid emergence of life shown by discovery of 3,700-million-year-old microbial structures. *Nature* **537**, 535–538.

Nutman AP, Bennett VC, Friend CRL, Van Kranendonk MJ, Rothacker L and Chivas AR (2019) Cross-examining Earth's oldest stromatolites: seeing through the effects of heterogeneous deformation, metamorphism and metasomatism affecting Isua (Greenland) ~3700 Ma sedimentary rocks. *Precambrian Research* **331**, 105347.

Oparin AI (1924) *El Origen de la Vida* (2015th ed.). Akal.

Orgel LE (1998) The origin of life – a review of facts and speculations. *Trends in Biochemical Sciences* **23**, 491–495.

Pérez-Rodríguez AE (2020) Estudio de la importancia de la energía de las ondas de choque atmosféricas debidas a la interacción de asteroides y cometas con la atmósfera terrestre primitiva, en la producción de compuestos orgánicos de interés astrobiológico. Universidad Nacional Autónoma de México. Available at http://132.248.9.195/ptd2020/noviembre/0805652/Index.html

Quirico E, Montagnac G, Lees V, McMillan PF, Szopa C, Cernogora G, Rouzaud JN, Simon P, Bernard JM, Coll P, Fray N, Minard RD, Raulin F, Reynard B and Schmitt B (2008) New experimental constraints on the composition and structure of tholins. *Icarus* **198**, 218–231.

Reeves EP and Fiebig J (2020) Abiotic synthesis of methane and organic compounds in earth's lithosphere. *Elements* **16**, 25–31.

Sagan C and Chyba C (1997) The Early Faint Sun Paradox: Organic Shielding of Ul traviolet-Labile Green house Gases. 276 (May).

Sagan C and Mullen G (1972) Earth and Mars: evolution of atmospheres and surface temperatures. *Science* **177**, 52–56.

Scattergood TW, McKay CP, Borucki WJ, Giver LP, van Ghyseghem H, Parris JE and Miller SL (1989). Production of organic compounds in plasmas: a comparison among electric sparks, laser-induced plasmas, and UV light. *Icarus* **81**, 413–428.

Schaefer L and Fegley B (2007) Outgassing of ordinary chondritic material and some of its implications for the chemistry of asteroids, planets, and satellites. *Icarus* **186**, 462–483.

Schaefer L and Fegley B (2010) Chemistry of atmospheres formed during accretion of the Earth and other terrestrial planets. *Icarus* **208**, 438–448.

Schaefer L and Fegley B (2017). Redox states of initial atmospheres outgassed on rocky planets and planetesimals. *The Astrophysical Journal* **843**, 120.

Schopf JW (2006) The first billion years: when did life emerge? *Elements* **2**, 229–233.

Segura A and Navarro-González R (2005) Production of low molecular weight hydrocarbons by volcanic eruptions on early Mars. *Origins of Life and Evolution of the Biosphere* **35**, 477–487.

Sugisaki R, Mimura K and Kato M (1994) Shock synthesis of light hydrocarbon gases from H2 and CO: its role in astrophysical processes. *Geophysical Research Letters* **21**, 1031–1034.

Trail D, Watson EB and Tailby ND (2011). The oxidation state of Hadean magmas and implications for early Earth's atmosphere. *Nature* **480**, 79–82.

Trainer MG, Pavlov AA, DeWitt HL, Jimenez JL, McKay CP, Toon OB and Tolbert MA (2006). Organic haze on Titan and the early Earth. *Proceedings of the National Academy of Sciences of the USA* **103**, 18035–18042.

Trigo-Rodriguez JM and Martín-Torres FJ (2012) Clues on the importance of comets in the origin and evolution of the atmospheres of Titan and Earth. *Planetary and Space Science* **60**, 3–9.

Urey HC (1952) On the early chemical history of the earth and the origin of life. *Proceedings of the National Academy of Sciences* **38**, 351–363.

Zahnle KJ (2006) Earth 's earliest atmosphere. *Elements* **2**, 217–222.

Zahnle K, Schaefer L and Fegley B (2010) Earth 's earliest atmospheres. *Cold Spring Harbor Perspectives in Biology* **2**, 1–17.

Zahnle KJ, Lupu R, Catling DC and Wogan N (2020) Creation and evolution of impact-generated reduced atmospheres of early earth. *The Planetary Science Journal* **1**, 1–11.

Zellner NEB (2017). Cataclysm no more: new views on the timing and delivery of lunar impactors. *Origins of Life and Evolution of Biospheres* **47**, 261–280.